J. Phase Equilib. Diffus. (2020) 41:207–217
https://doi.org/10.1007/s11669-020-00809-1

Experimental Liquidus Studies of the ZnO-"$CuO_{0.5}$" and ZnO-"$CuO_{0.5}$"-SiO_2 Liquidus in Equilibrium with Cu-Zn Metal

M. Shevchenko[1] · **E. Jak**[1]

Submitted: 6 March 2020 / in revised form: 7 April 2020 / Published online: 7 May 2020

Abstract Phase equilibria in the ZnO-"$CuO_{0.5}$"-SiO_2 system have been investigated at 1403-1948 K (1130-1675 °C) for oxide liquid in equilibrium with Cu-Zn metal (> 99% Cu) and solid oxide phases: (a) tridymite or cristobalite SiO_2; (b) willemite Zn_2SiO_4; (c) zincite ZnO; and (d) cuprite Cu_2O. Two-liquid immiscibility range in the high-SiO_2 slags has also been studied. High-temperature equilibration on primary phase (SiO_2, Cu_2O), inert metal (platinum-iridium wire), or ceramic (Al_2O_3 for high-Cu_2O slags) substrates, followed by quenching and direct measurement of Zn, Cu, Si and possible impurities (Al, Pt, Ir) concentrations in the phases with the electron probe x-ray microanalysis (EPMA) has been used to accurately characterize the system in equilibrium with metal. All results are projected onto the ZnO-"$CuO_{0.5}$"-SiO_2 plane for presentation purposes.

Keywords copper · phase diagrams · silica · slags · zinc

1 Introduction

The study of the ZnO-"$CuO_{0.5}$"-SiO_2 system represents an important part of the overall integrated thermodynamic modelling and experimental research program for the multicomponent Pb-Zn-Fe-Cu-Si-Ca-Al-Mg-O system. Its study provides essential thermodynamic information to predict distribution of Cu in ZnO-rich slags and Zn in Cu_2O-rich slags, the importance of this is increasing due to development of pyrometallurgical recycling of complex secondary materials, such as waste electrical and electronic equipment (WEEE), and other common materials containing brass.

A preliminary study of the liquidus surface of the ZnO-$CuO_{0.5}$-CuO-SiO_2 system has been carried out by Xia and Taskinen.[1-3] Most of the data in that study were obtained in air, which is far from the pyrometallurgical processing conditions; only two points at 1200 °C have been obtained in the ternary region in equilibrium with metal. No other studies have been found in literature.

2 Experimental Technique and Procedure

The experimental procedure and apparatus have been described in detail in previous publications by the authors.[4-6] The initial mixtures were prepared by mixing high-purity powders Cu_2O (99.9 wt.% purity) supplied by Heysham, Great Britain, and ZnO (99.8 wt.% purity), SiO_2 (99.9 wt.% purity), and Cu (99.9 wt.% purity) supplied by Alfa Aesar, MA, USA. ZnO-SiO_2 (1:1 mol. ratio) master-slag was used in several open substrate experiments to reduce evaporation loss of ZnO. The mixtures were pressed into pellets using a tool steel die. Less than 0.5 g of mixture was used in each equilibration experiment. The initial compositions of the mixtures were selected so that one or more crystalline phases would be present in equilibrium with liquid slag and approximately 10 vol.% metal. The volume fraction of solids was targeted to be below 50 vol.%, and preferably about 10 vol.%, to achieve rapid equilibration and useful outcomes from quenching (it was found that the solids serve as heterogeneous nucleation centers, and the minimum distance between them should

✉ M. Shevchenko
m.shevchenko@uq.edu.au

[1] Pyrometallurgy Innovation Centre (PYROSEARCH), The University of Queensland, Brisbane, QLD 4072, Australia

exceed 10-20 micron to ensure that amorphous slag of uniform composition, unaffected by dendritic crystal growth, is obtained). An iterative procedure involving preliminary experiments was often needed to achieve the targeted proportions of the phases for a given final temperature and composition.

Four types of substrates were used for equilibration, depending on the conditions:

1. Silica ampoules (5 cm long, 1.3 cm outer diameter, 0.1 cm thick wall, 99.999% SiO_2, supplied by GY, Jiangsu, China) sealed under vacuum ($\sim$ 0.001 atm), or with small holes, or open silica crucibles for the samples in the cristobalite/tridymite primary phase fields. Sealing allowed preventing the loss of the volatile Zn from the system, as well as oxidation of the samples by residual oxygen in the gas atmosphere. Pelletizing of the powder mixture was used to avoid the presence of loose powder particles, which could be preferentially extracted from the ampoule during evacuation. The protection against Zn evaporation is increased in the order open crucible < ampoule with hole < sealed ampoule. However, the quenching speed decreases in the same order. Experiments on open substrates were limited to low temperatures (up to 1400 °C), because at higher temperatures the loss of Zn becomes too fast to allow reasonable equilibration time.
2. Willemite (Zn_2SiO_4)-covered SiO_2 crucibles—prepared by melting ZnO-SiO_2 mixture on the SiO_2 substrate. However, willemite layer was usually not dense enough to prevent significant diffusion of SiO_2 from crucible to slag, so this assemblage did not work for low-SiO_2 ranges. Direct diffusion through willemite solid layer is considered unlikely. Possible diffusion is due to cracks in the willemite layer. Since they were not found in the given experiments, and the liquid composition was measured at variable distances from the substrate and found to be homogeneous, these experiments were included as successful.
3. Al_2O_3 crucibles (99.7%, 8 mm inner diameter, 15 mm height, supplied by Xiamen Wintrustek, Fujian, China) were used only in the range within or close to the ZnO-Cu_2O subsystem, since it was found that high-Cu_2O, low-SiO_2 slags have low solubility of Al_2O_3 ($\sim$ 1%), while difficult to handle on other substrates due to high fluidity and fast loss of Zn. The layer of $ZnAl_2O_4$ was found to be dense with no cracks. No detached $ZnAl_2O_4$ particles were present. Also, liquid and zincite measured at variable distances from the substrate were found to have the same composition. This indicates that liquid and zincite have reached saturation with Al_2O_3 within the first minutes during formation of $ZnAl_2O_4$, and further diffusion is likely to be slow.
4. Iridium (99.99%) or platinum-30% iridium wire (supplied by Huanya, Jiangsu, China) substrate was used for the samples in the willemite, zincite and cuprite primary phase fields. Contamination of Cu metal by platinum (up to 30%) and iridium (up to 3%), and probability of the wire breaking are the limitations of this substrate type. As soon as there is > 70 wt.% Cu in metal (> 90 mol.% since the impurities Ir and Pt are heavy), the effect on phase equilibria due to formation of Cu^{2+} in slag can be neglected.

All equilibration experiments were carried out in a vertical reaction tube (impervious recrystallized alumina, 30-mm inner diameter) within an electrical resistance (SiC or $MoSi_2$) heated furnace. The samples were placed immediately adjacent to a working thermocouple in a recrystallized alumina sheath in the uniform hot zone of the furnace to monitor the actual sample temperature. The working thermocouple was calibrated against a standard thermocouple (supplied by the National Measurement Institute of Australia, NSW, Australia). The overall absolute temperature accuracy of the experiment was estimated to be $\pm$ 3 K.

The samples were suspended in the hot zone of the furnace by Kanthal support wire (Fe-Cr-Al alloy, 0.7 or 1-mm diameter). For temperatures higher than 1773 K (1500 °C), a 20-25 cm Mo or Pt-Rh wire was used to extend the support, so that the Kanthal wire is not in the hot zone. The samples were pre-melted for 5-10 min at 20-100 K above the equilibration temperature, to form a homogeneous liquid slag. Some samples in the ranges where even a small additional increase in temperature could cause failure due to evaporation of Zn or broken substrate were not premelted. Premelt was followed by equilibration at the final target temperature for the required time. A compromise had to be found between longer time for better equilibration and the risk to lose the volatile component or destroy the substrate. The analysis of various parts of the samples did not indicate significant non-equilibrium. Shorter times were limited to low-SiO_2 (low viscosity) or high-temperature (high reaction rate) ranges. At the end of the equilibration process, the samples were released and rapidly quenched into the $CaCl_2$ brine (< 253 K (− 20 °C)). The samples were then washed thoroughly in water and ethanol before being dried on a hot plate, mounted in epoxy resin, and cross-sectioned using conventional metallographic polishing techniques.

The samples were examined by optical microscopy, carbon-coated, and the phase compositions were measured using an electron probe x-ray microanalysis technique with wavelength dispersive detectors (JEOL 8200L EPMA;

Japan Electron Optics Ltd., Tokyo, Japan). The EPMA was operated with 15 kV accelerating voltage and 20 nA probe current. Copper (Cu), quartz (SiO_2), wollastonite ($CaSiO_3$), corundum (Al_2O_3) (supplied by Charles M. Taylor Co., Stanford, CA), and zincite (sintered from 99.8% ZnO powder) standards were used for calibration of EPMA. The concentrations of metal cations were measured with EPMA; no information on the oxidation states of the metal cations was obtained. Copper oxide concentrations were recalculated as Cu_2O for presentation purposes only; this oxidation state was selected according to the information on the slags in equilibrium with metal in the Cu-Si-O system.[7] The molar ratios of the oxides were used in the graphical presentation of the data.

The standard Duncumb–Philibert atomic number, absorption, and fluorescence (ZAF) correction supplied by JEOL[8-10] was used. The standard ZAF correction was further improved following an approach similar to the one previously described.[11-13] The accuracy of ZAF correction for the "$CuO_{0.5}$"-SiO_2 system has been checked recently,[14] using dehydrated natural dioptase ($CuSiO_3$) as a reference material of fixed composition; overestimation of SiO_2 concentration by 1.8% was observed. In the ZnO-SiO_2 system, willemite Zn_2SiO_4 was used as a reference material.[15,16] The combined correction formulas for the ZnO-"$CuO_{0.5}$"-SiO_2 slags are:

$$x_{SiO_2}^{corrected} = x_{SiO_2} - 0.07 \cdot x_{SiO_2} x_{CuO_{0.5}} - 0.07 \cdot x_{SiO_2} x_{ZnO} \quad \text{(Eq 1)}$$

$$x_{CuO_{0.5}}^{corrected} = x_{CuO_{0.5}} + 0.07 \cdot x_{SiO_2} x_{CuO_{0.5}} \quad \text{(Eq 2)}$$

$$x_{ZnO}^{corrected} = x_{ZnO} + 0.07 \cdot x_{SiO_2} x_{ZnO} \quad \text{(Eq 3)}$$

Same correction is used for previous data obtained in the "$CuO_{0.5}$"-SiO_2 system.[17]

The ability to quench the liquid slag phase to ambient temperature without the onset of crystallization was found to depend on the composition of the slag and the equilibration temperature. Significant problems were observed with low-silica slags in the zincite primary phase field, where the glassy homogeneous areas were only a small proportion of the melt, believed to be formed at the surfaces directly contacting the quenching medium. For these samples the approach taken to obtain accurate, repeatable, and objective measurements of the average compositions of the liquid slag phase by the use of EPMA was similar to that described by Nikolic et al.[18]: an average of at least 20 points in the best quenched area (usually, near the surface) was used, additionally controlled by standard deviation of composition not exceeding 1 mol.%. In cases where melt crystallization was rapid, the experiments were repeated until an area of sufficiently well-quenched microstructure was found. Increasing the probe diameter to 20-50 micron resulted in reduced variability of the measured liquid slag compositions, while zero probe diameter was only used for solid phases.

Special experiments were undertaken in the present study with the 50-200 micron size grains of pure unreacted quartz pressed together with the Cu and ZnO powders, and crushed sintered zincite with the Cu powder at room temperature (unreacted couples). Apparent 1.05 mol.% "$CuO_{0.5}$" and 0.82 mol.% ZnO are observed due to the secondary x-ray fluorescence in pure quartz grains surrounded by Cu and ZnO, respectively. Apparent 1.03 mol.% "$CuO_{0.5}$" is observed in pure zincite grains surrounded by Cu. It was found in the previous studies of other systems involving elements with high-energy (> 5 keV) lines (Fe, Cu, Zn)[14,16,19] that the secondary fluorescence effect can be observed over large distances (> 100 micron). This is much more than the typical size of the observed solid particles in the present system (10-40 micron). Therefore, the x-rays formed in these particles have low probability not to exit them into the surrounding slag matrix. This allows to assume that the geometry effect was comparable in all observed cases. The following correction for the secondary x-ray fluorescence (similar to [14,16,19]) therefore has been developed and applied in the present study to the compositions of tridymite and cristobalite measured by EPMA:

$$x(CuO_{0.5} \text{ in } SiO_2)^{corr} = x(CuO_{0.5} \text{ in } SiO_2)^{initial} - 0.0093 * \text{wt. fraction}(CuO_{0.5} \text{ in slag}),$$

$$x(ZnO \text{ in } SiO_2)^{corr} = x(ZnO \text{ in } SiO_2)^{initial} - 0.0082 \text{ wt. fraction}(ZnO \text{ in slag});$$

for zincite:

$$x(CuO_{0.5} \text{ in } ZnO)^{corr} = x(CuO_{0.5} \text{ in } ZnO)^{initial} - 0.0092 * \text{wt. fraction}(CuO_{0.5} \text{ in slag}),$$

for willemite:

$$x(CuO_{0.5} \text{ in } Zn_2SiO_4)^{corr} = x(CuO_{0.5} \text{ in } Zn_2SiO_4)^{initial} - 0.0092 * \text{wt. fraction}(CuO_{0.5} \text{ in slag}).$$

According to these formulae, most of observed solubility of ZnO in tridymite and cristobalite, and "$CuO_{0.5}$" in tridymite, cristobalite and willemite are due to the effect of secondary x-ray fluorescence. However, only part of observed "$CuO_{0.5}$" in zincite can be attributed to fluorescence, while most of it is a real solubility.

The effect of secondary fluorescence on slag composition measurement is mostly accounted by the corrections using willemite and dioptase reference standards. One exception is that fake increase of Cu in slag can be found near large Cu particles—these locations were avoided during analysis.

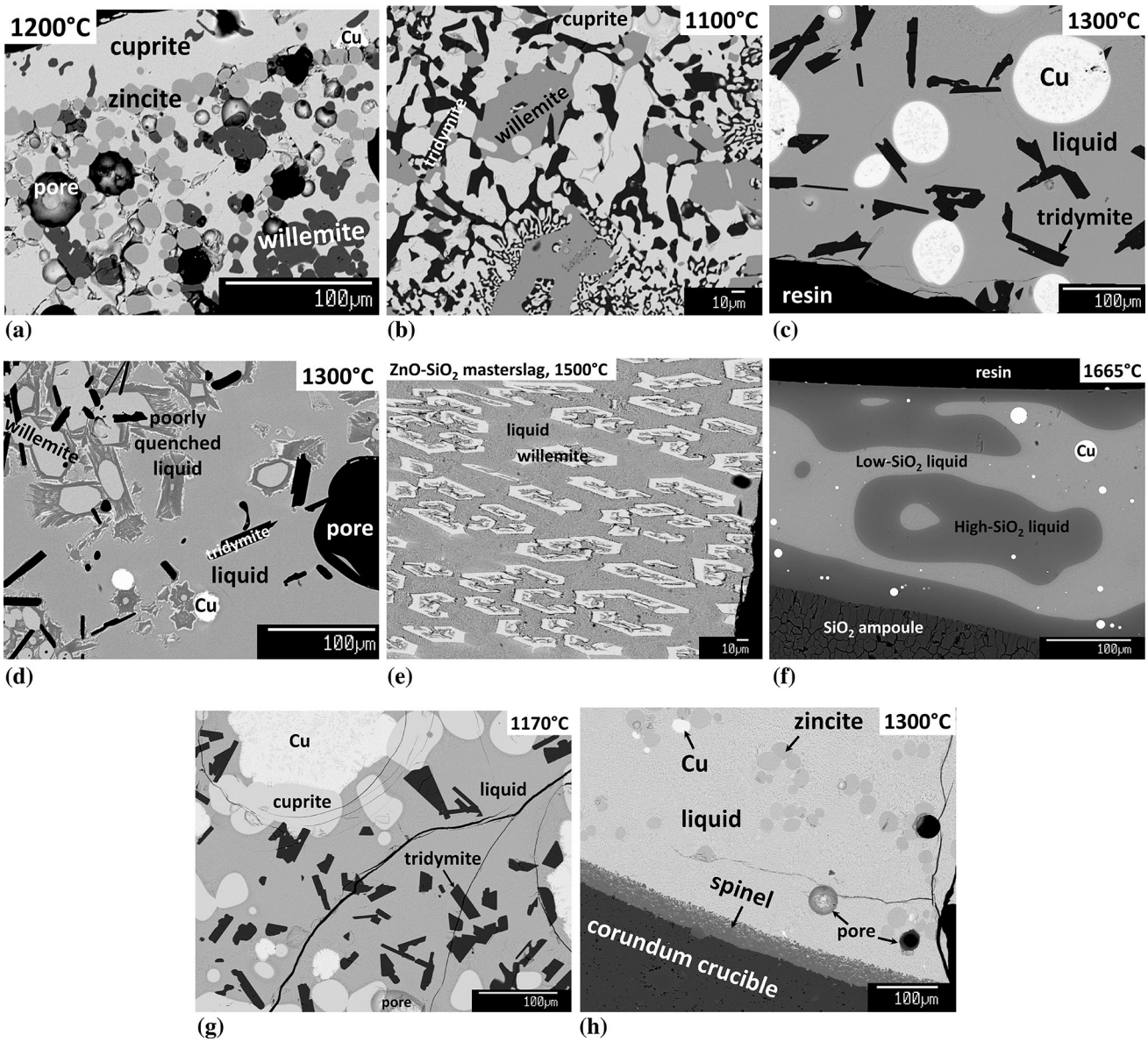

Fig. 1 Microstructures of quenched samples of the ZnO-"$CuO_{0.5}$"-SiO_2 system in equilibrium with metallic Cu. (a) Willemite (Zn_2SiO_4) + zincite (ZnO) + cuprite (Cu_2O) + Cu (subsolidus), (b) Willemite (Zn_2SiO_4) + tridymite (SiO_2) + cuprite (Cu_2O) + Cu (subsolidus)* (* Cu is present in other parts of the sample), (c) Liquid + tridymite (SiO_2) + Cu, (d) Liquid (with areas of dendritic growth) + tridymite (SiO_2) + willemite (Zn_2SiO_4) + Cu, (e) Masterslag (molten ZnO + SiO_2 mixture), with willemite precipitation, (f) Two immiscible liquids + Cu, (g) Liquid + cuprite (Cu_2O) + tridymite (SiO_2) + Cu, (h) Liquid + zincite (ZnO) + Cu + spinel ($ZnAl_2O_4$) on corundum (Al_2O_3)

3 Results and Discussion

Typical microstructures are shown in Fig. 1. The phase compositions with standard deviations are reported in Table 1. The liquidus surface of the ZnO-"$CuO_{0.5}$"-SiO_2 system in equilibrium with Cu(-Zn) metal is presented in Fig. 2, and ZnO-"$CuO_{0.5}$" system in equilibrium with Cu(-Zn) metal—in Fig. 3.

The "$CuO_{0.5}$"-ZnO system in equilibrium with metal is characterised by cuprite-zincite eutectic at 1206 ± 3 °C and steeply rising ZnO liquidus (ZnO in slag does not increase significantly by 1400 °C), indicating strong positive deviations from ideal solution behaviour (Fig. 3). In the present study, Al_2O_3 dissolves in both liquid and zincite, and is expected to stabilize both approximately equally. We acknowledge that this is not true Cu_2O-ZnO-SiO_2 system, but only the closest approximation of it achieved so far (in this problematic range of compositions). Plotted points are projections. Two immiscible liquids formation in the central range of the "$CuO_{0.5}$"-ZnO system

Table 1 Experimental points on the liquidus surface with compositions of phases in the ZnO-"$CuO_{0.5}$"-SiO_2 system in equilibrium with metal

No.	*T*, °C	Substrate	Premelt *T*, °C	Time, h	Phase	Composition, mol.%		
						SiO_2	ZnO/Zn	$CuO_{0.5}$/Cu
Tridymite and cristobalite (SiO_2) liquidus								
1	1140	SiO_2 amp	1240	0.25 + 18	Liquid	24.7 ± 0.8	9.5 ± 1.3	65.8 ± 2.0
					Tridymite	99.6 ± 0.13	0.13 ± 0.06	0.26 ± 0.09
2	1150	SiO_2 amp + hole	1240	0.25 + 2	Liquid	23.9 ± 0.11	9.1 ± 0.3	67.1 ± 0.3
					Tridymite	99.7 ± 0.17	0.11 ± 0.05	0.23 ± 0.14
3	1200	SiO_2 amp + hole	1240	0.25 + 2	Liquid	24.1 ± 0.2	8.0 ± 0.3	67.9 ± 0.4
					Tridymite	99.5 ± 0.16	0.12 ± 0.05	0.35 ± 0.14
4	1200	SiO_2 open crucible	1250	0.25 + 1.5	Liquid	34.6 ± 0.13	19.4 ± 0.4	46.0 ± 0.4
					Tridymite	99.3 ± 0.1	0.65 ± 0.12	0.08 ± 0.02
5	1200	SiO_2 open crucible	1250	0.25 + 1.5	Liquid	31.7 ± 0.3	15.7 ± 0.5	52.6 ± 0.7
					Tridymite	99.5 ± 0.1	0.26 ± 0.04	0.25 ± 0.07
6	1200	SiO_2 open crucible	1250	0.25 + 1.5	Liquid	32.2 ± 0.2	17.7 ± 0.5	50.1 ± 0.6
					Tridymite	99.5 ± 0.1	0.26 ± 0.04	0.25 ± 0.07
7	1300	SiO_2 open crucible	1320	0.25 + 1.5	Liquid	42.3 ± 0.16	31.3 ± 0.4	26.3 ± 0.5
					Tridymite	99.1 ± 0.12	0.8 ± 0.1	0.1 ± 0.08
8	1300	SiO_2 open crucible	1320	0.25 + 1.5	Liquid	30.4 ± 0.17	11.0 ± 0.3	58.6 ± 0.4
					Tridymite	99.6 ± 0.2	0.14 ± 0.02	0.28 ± 0.2
9	1300	SiO_2 open crucible	1320	0.25 + 1.5	Liquid	35.5 ± 0.3	17.2 ± 0.5	47.3 ± 0.8
					Tridymite	99.4 ± 0.17	0.34 ± 0.08	0.3 ± 0.09
10	1300	SiO_2 open crucible	1320	0.25 + 1.5	Liquid	37.6 ± 0.5	21.1 ± 0.5	41.3 ± 0.8
					Tridymite	99.4 ± 0.17	0.34 ± 0.08	0.3 ± 0.09
					Metal	0	0.14 ± 0.02	99.86 ± 0.02
11	1330	SiO_2 amp + hole	No	2	Liquid	30.0 ± 0.5	7.8 ± 0.7	62.2 ± 1.0
					Tridymite	99.5 ± 0.03	0.16 ± 0.03	0.3 ± 0.03
12	1350	SiO_2 open crucible	1380	0.25 + 1.5	Liquid	44.9 ± 0.16	35.0 ± 0.3	20.1 ± 0.2
					Tridymite	99.2 ± 0.11	0.7 ± 0.04	0.12 ± 0.07
13	1350	SiO_2 open crucible	1380	0.25 + 1.5	Liquid	44.8 ± 0.06	36.7 ± 0.13	18.5 ± 0.13
					Tridymite	99.2 ± 0.11	0.7 ± 0.04	0.12 ± 0.07
					Metal	0	0.13 ± 0.08	99.87 ± 0.08
14	1400	SiO_2 open crucible	1410	0.25 + 1.5	Liquid	34.0 ± 0.2	10.1 ± 0.4	55.9 ± 0.3
					Tridymite	99.6 ± 0.2	0.13 ± 0.06	0.23 ± 0.15
15	1400	SiO_2 open crucible	1410	0.25 + 1.5	Liquid	40.5 ± 0.5	18.4 ± 0.8	41.1 ± 1.2
					Tridymite	99.4 ± 0.08	0.3 ± 0.06	0.26 ± 0.06
16	1400	SiO_2 amp	1420	0.2 + 3	Liquid	46.6 ± 0.14	42.9 ± 0.14	10.5 ± 0.11
					Tridymite	99.0 ± 0.02	0.7 ± 0.2	0.27 ± 0.2
					Metal	0	0.28 ± 0.14	99.72 ± 0.14
17	1500	SiO_2 amp	1520	0.2 + 2	Liquid	24.1 ± 0.4	0	75.9 ± 0.4
					Cristobalite	99.7	0	0.3
18	1500	SiO_2 amp	1520	0.2 + 2	Liquid	42.2 ± 0.2	12.2 ± 0.2	45.6 ± 0.3
					Cristobalite	99.4 ± 0.03	0.2 ± 0.01	0.4 ± 0.02
19	1500	SiO_2 amp	No	1	Liquid	50.5 ± 0.13	24.6 ± 0.15	24.9 ± 0.17
					Cristobalite	99.0 ± 0.06	0.5 ± 0.06	0.5 ± 0.03
20	1500	SiO_2 amp	1520	0.2 + 2	Liquid	50.3 ± 0.16	34.7 ± 0.18	15.0 ± 0.12
					Cristobalite	99.2 ± 0.02	0.6 ± 0.08	0.2 ± 0.06
					Metal	0	0.25 ± 0.06	99.75 ± 0.06
21	1550	SiO_2 open crucible	1570	0.2 + 1	Liquid	27.7 ± 0.4	0	72.3 ± 0.4
					Cristobalite	99.7	0	0.3
22	1600	SiO_2 amp	No	1	Liquid	32.5 ± 0.6	0	67.5 ± 0.6
					Cristobalite	99.7	0	0.3
23	1600	SiO_2 amp	No	1	Liquid	39.9 ± 0.5	4.6 ± 0.12	55.5 ± 0.4
					Cristobalite	99.5	0.1	0.4

Table 1 continued

No.	*T*, °C	Substrate	Premelt *T*, °C	Time, h	Phase	Composition, mol.%		
						SiO_2	ZnO/Zn	$CuO_{0.5}$/Cu
24	1600	SiO_2 amp	No	1	Liquid	51.3 ± 0.1	12.1 ± 0.1	36.6 ± 0.16
					Cristobalite	99.4	0.3	0.3
25	1600	SiO_2 amp	No	1	Liquid	55.3 ± 0.15	17.2 ± 0.14	27.4 ± 0.2
					Cristobalite	99.3 ± 0.13	0.4 ± 0.09	0.3 ± 0.06
26	1600	SiO_2 amp	No	1	Liquid	57.2 ± 0.3	29.2 ± 0.16	13.6 ± 0.15
					Cristobalite	99.0 ± 0.05	0.8 ± 0.06	0.2 ± 0.05
					Metal	0	0.21 ± 0.02	99.79 ± 0.02
27	1630	SiO_2 amp	1640	0.1 + 1	Liquid	56.8 ± 0.15	12.7 ± 0.18	30.5 ± 0.19
					Cristobalite	99.4 ± 0.08	0.2 ± 0.05	0.4 ± 0.07
28	1642	SiO_2 amp	1650	0.1 + 1	Liquid	73.9 ± 0.3	14.8 ± 0.2	11.3 ± 0.13
					Cristobalite	99.5 ± 0.06	0.3 ± 0.03	0.2 ± 0.08
					Metal	0	0.23 ± 0.02	99.77 ± 0.02
29	1650	SiO_2 amp	No	0.7	Liquid	37.0 ± 0.4	0	63.0 ± 0.4
					Cristobalite	99.7	0	0.3
30	1650	SiO_2 amp	1657	0.2 + 1	Liquid	87.3 ± 0.8	5.3 ± 0.3	7.4 ± 0.5
					Cristobalite	~ 100	n.a.	
					Metal	0	0.4	99.6
31	1658	SiO_2 amp	1665	0.1 + 1	Liquid	90.6 ± 0.4	6.6 ± 0.3	2.8 ± 0.12
					Cristobalite	~ 100	n.a.	
					Metal	0	0.4 ± 0.16	99.6 ± 0.16
32	1660	SiO_2 amp	No	0.7	Liquid	91.6 ± 0.9	1.9 ± 0.12	6.5 ± 0.8
					Cristobalite	~ 100	n.a.	
33	1665	SiO_2 amp	No	0.7	Liquid	93.3 ± 0.9	4.7 ± 0.6	2.0 ± 0.3
					Cristobalite	~ 100	n.a.	
34	1677	SiO_2 amp	No	0.5	Liquid1	38.4 ± 0.2	0	61.6 ± 0.2
					Liquid2	95.1 ± 0.1	0	4.9 ± 0.1
					Cristobalite	99.6	0	0.4
2 liquids								
35	1658	SiO_2 amp	1665	0.1 + 1	Liquid1	74.1 ± 0.5	18.9 ± 0.4	7.0 ± 0.14
					Liquid2	86.1 ± 0.6	9.9 ± 0.5	4.0 ± 0.16
36	1660	SiO_2 amp	No	0.7	Liquid1	55.4 ± 1.8	7.9 ± 0.3	36.7 ± 1.6
					Liquid2	79.6 ± 0.5	5.0 ± 0.09	15.4 ± 0.4
37	1665	SiO_2 amp	No	0.7	Liquid1	70.7 ± 0.5	21.4 ± 0.4	7.9 ± 0.16
					Liquid2	87.6 ± 0.4	8.8 ± 0.3	3.6 ± 0.11
Tridymite + cuprite boundary								
38	1150	SiO_2 amp	1200;	0.2 + 1+4	Liquid	24.3 ± 0.2	8.5 ± 0.2	67.2 ± 0.4
			1100		Tridymite	99.8	0.1	0.1
					Cuprite	0.0	0.1 ± 0.01	99.9 ± 0.02
39	1160	SiO_2 amp	1200;	0.2 + 1+4	Liquid	22.1 ± 0.4	5.3 ± 0.2	73.8 ± 0.5
			1100		Tridymite	99.8	0.1	0.1
					Cuprite	0.0	0.9 ± 0.07	99.9 ± 0.07
40	1170	SiO_2 amp	1200;	0.2 + 1+3	Liquid	18.3 ± 0.3	4.0 ± 0.1	77.7 ± 0.3
			1100		Tridymite	99.7 ± 0.15	0.1 ± 0.04	0.2 ± 0.11
					Cuprite	0.05 ± 0.02	0.15 ± 0.03	99.8 ± 0.04
Willemite + cuprite boundary								
41	1160	Pt-30%Ir wire	1165	0.2 + 2	Liquid	23.1 ± 0.2	12.4 ± 0.2	64.5 ± 0.3
					Willemite	33.3 ± 0.11	66.0 ± 0.01	0.7 ± 0.11
					Cuprite	0.0	0.2 ± 0.03	99.8 ± 0.03

Table 1 continued

No.	*T*, °C	Substrate	Premelt *T*, °C	Time, h	Phase	Composition, mol.%		
						SiO_2	ZnO/Zn	$CuO_{0.5}$/Cu
Tridymite + willemite boundary								
42	1140	SiO_2 amp + hole	1240	0.25 + 2.5	Liquid	26.8 ± 0.3	12.6 ± 0.4	60.6 ± 0.6
					Tridymite	99.6 ± 0.03	0.36 ± 0.4	<0.1
					Willemite	32.6 ± 0.14	67.2 ± 0.2	0.22 ± 0.16
43	1150	Z_2S* + SiO_2 open crucible	1240	0.25 + 2	Liquid	28.2 ± 0.3	13.5 ± 0.4	58.3 ± 0.6
					Tridymite	99.3	0.4	0.3
					Willemite	33.1 ± 0.16	66.7 ± 0.3	0.24 ± 0.3
44	1200	SiO_2 open crucible	1250	0.25 + 1.5	Liquid	34.9 ± 0.19	20.2 ± 0.3	44.8 ± 0.4
					Tridymite	99.3 ± 0.1	0.65 ± 0.12	0.08 ± 0.02
					Willemite	33.4 ± 0.06	65.7 ± 0.3	0.8 ± 0.3
45	1250	Z_2S + SiO_2 open crucible	1260	0.25 + 1.5	Liquid	39.3 ± 0.2	27.2 ± 0.19	33.5 ± 0.3
					Tridymite	~ 100	n.a.	n.a.
					Willemite	32.6 ± 0.16	66.9 ± 0.2	0.55 ± 0.2
46	1300	SiO_2 open crucible	1320	0.25 + 1.5	Liquid	42.7 ± 0.14	32.3 ± 0.2	25.0 ± 0.2
					Tridymite	99.1 ± 0.12	0.84 ± 0.1	0.09 ± 0.08
					Willemite	33.4 ± 0.12	66.1 ± 0.12	0.53 ± 0.18
47	1380	SiO_2 amp	1410	0.2 + 2	Liquid	45.9 ± 0.2	44.2 ± 0.18	9.9 ± 0.1
					Tridymite	98.8	1.1	0.1
					Willemite	33.0 ± 0.1	66.8 ± 0.12	0.2 ± 0.15
Willemite (Zn_2SiO_4) liquidus								
48	1200	Ir plate	1240	0.25 + 1.5	Liquid	11.0 ± 0.4	9.4 ± 0.5	79.6 ± 0.8
					Willemite	33.0 ± 0.18	66.4 ± 0.5	0.65 ± 0.6
49	1250	Z_2S + SiO_2 open crucible	1260	0.25 + 1.5	Liquid	36.9 ± 0.3	26.4 ± 0.4	36.7 ± 0.5
					Willemite	32.6 ± 0.16	66.9 ± 0.2	0.55 ± 0.2
50	1250	Pt-30%Ir wire	1280	0.2 + 1.5	Liquid	16.3 ± 0.3	15.4 ± 0.5	68.3 ± 0.7
					Willemite	33.0 ± 0.08	66.8 ± 0.13	0.18 ± 0.09
51	1250	Pt-30%Ir wire	1280	0.2 + 1.5	Liquid	19.1 ± 0.6	17.6 ± 0.5	63.3 ± 1.0
					Willemite	33.0 ± 0.18	66.7 ± 0.3	0.3 ± 0.13
52	1250	Pt-30%Ir wire	1280	0.2 + 1.5	Liquid	25.4 ± 0.3	22.1 ± 0.3	52.5 ± 0.5
					Willemite	32.9 ± 0.06	66.7 ± 0.3	0.45 ± 0.3
53	1300	Pt-30%Ir wire	1320	0.2 + 1	Liquid	23.5 ± 0.15	28.7 ± 0.3	47.8 ± 0.3
					Willemite	33.0 ± 0.13	66.7 ± 0.3	0.28 ± 0.4
54	1300	Pt-30%Ir wire	1320	0.2 + 1	Liquid	31.3 ± 0.13	30.1 ± 0.15	38.5 ± 0.2
					Willemite	32.9 ± 0.12	66.8 ± 0.17	0.34 ± 0.19
55	1300	Pt-30%Ir wire	1320	0.2 + 1	Liquid	32.2 ± 0.08	30.8 ± 0.11	37.0 ± 0.03
					Willemite	32.9 ± 0.12	66.8 ± 0.17	0.34 ± 0.19
56	1350	Pt-30%Ir wire	No	0.3	Liquid	21.1 ± 0.09	45.6 ± 0.3	33.3 ± 0.3
					Willemite	33.2 ± 0.09	66.6 ± 0.14	0.2 ± 0.18
Willemite (Zn_2SiO_4) + zincite (ZnO) boundary								
57	1210	Pt-30%Ir wire	1230	0.2 + 1	Liquid	2.5 ± 0.07	7.8 ± 0.2	89.7 ± 0.2
					Willemite	33.1 ± 0.08	66.2 ± 0.3	0.7 ± 0.4
					Zincite	0.02 ± 0.02	98.1 ± 0.04	1.9 ± 0.02
58	1250	Pt-30%Ir wire	1300	0.25 + 1.5	Liquid	4.8 ± 0.13	11.9 ± 0.4	83.3 ± 0.5
					Willemite	33.1 ± 0.11	66.5 ± 0.3	0.45 ± 0.2
					Zincite	0.07 ± 0.03	97.5 ± 0.3	2.4 ± 0.3
59	1300	Pt-30%Ir wire	1320	0.25 + 1.5	Liquid	11.5 ± 0.3	26.0 ± 0.5	62.6 ± 0.7
					Willemite	32.8 ± 0.16	67.0 ± 0.5	0.18 ± 0.4
					Zincite	0.11 ± 0.03	97.9 ± 0.18	1.9 ± 0.17
60	1330	Pt-30%Ir wire	No	0.3	Liquid	16.3 ± 0.3	36.8 ± 0.3	46.9 ± 0.6
					Willemite	33.1 ± 0.12	66.7 ± 0.12	0.2 ± 0.14
					Zincite	0.15 ± 0.03	97.7 ± 0.4	2.1 ± 0.4

Table 1 continued

No.	*T*, °C	Substrate	Premelt *T*, °C	Time, h	Phase	Composition, mol.%		
						SiO_2	ZnO/Zn	$CuO_{0.5}$/Cu
Subsolidus								
61	1200	Ir wire	1240	0.25 + 1.5	Willemite	33.0 ± 0.18	66.0 ± 0.6	0.9 ± 0.6
				**	Zincite	0.03 ± 0.03	97.3 ± 0.7	2.7 ± 0.7
					Cuprite	0.00	0.22 ± 0.1	99.78 ± 0.1
62	1100	SiO_2 open crucible	1240	0.25 + 2	Tridymite	99.5 ± 0.16	0.13 ± 0.13	0.37 ± 0.22
					Willemite	33.4 ± 0.12	65.2 ± 0.14	1.4 ± 0.05
					Cuprite	0.01 ± 0.01	0.19 ± 0.12	99.8 ± 0.12
63	1130	SiO_2 open crucible	1240	0.25 + 2.5	Tridymite	99.7 ± 0.2	0.15 ± 0.06	0.19 ± 0.2
					Willemite	32.8 ± 0.18	66.7 ± 0.4	0.56 ± 0.4
					Cuprite		n.a.	~ 100

No.	*T*, °C	Substrate	Premelt *T*, °C	Time, h	Phase	Corrected mol.%			
						$AlO_{1.5}$	SiO_2	ZnO	$CuO_{0.5}$
Zincite (ZnO) liquidus, on $ZnAl_2O_4$									
64	1300	Al_2O_3 open crucible	No	1	Liquid	1.27 ± 0.07	4.2 ± 0.2	12.3 ± 1.1	83.5 ± 1.2
					Zincite	2.2 ± 0.3	0.04 ± 0.01	94.5 ± 0.5	3.2 ± 0.2
					Spinel	68.9	0.24	28.7	2.21
65	1300	Al_2O_3 open crucible	No	1	Liquid	0.39 ± 0.03	0.0	4.8 ± 0.3	95.2 ± 0.3
					Zincite	2.3 ± 0.3	0.0	94.4 ± 0.5	3.3 ± 0.7
					Spinel	69.0	0.0	30.6	0.35
66	1400	Al_2O_3 open crucible	No	0.5	Liquid	0.63 ± 0.06	0.0	5.2 ± 0.6	94.8 ± 0.6
					Zincite	3.0 ± 0.16	0.0	93.1 ± 0.5	3.9 ± 0.4
					Spinel	68.5	0.0	30.7	0.82
67	1300	Al_2O_3 open crucible	No	0.7	Liquid	0.84 ± 0.06	2.3 ± 0.06	10.0 ± 0.5	87.7 ± 0.5
					Zincite	2.4 ± 0.15	0.04 ± 0.03	94.1 ± 0.5	3.5 ± 0.4
					Spinel	n.a.			
68	1400	Al_2O_3 open crucible	No	0.35	Liquid	1.43 ± 0.07	2.4 ± 0.06	12.7 ± 1.0	84.8 ± 1.1
					Zincite	3.2 ± 0.01	0.03 ± 0.02	92.8 ± 0.01	3.9 ± 0.02
					Spinel	70.0	0.27	28.7	0.96
69	1300	Al_2O_3 open crucible	No	0.7	Liquid	1.78 ± 0.06	6.8 ± 0.3	16.5 ± 0.8	76.7 ± 0.7
					Zincite	1.45 ± 0.9	0.07 ± 0.01	95.8 ± 1.8	2.6 ± 0.9
					Spinel	n.a.			
70	1400	Al_2O_3 open crucible	No	0.35	Liquid	3.2 ± 0.07	6.4 ± 0.2	23.5 ± 1.7	70.1 ± 1.7
					Zincite	n.a.			
					Spinel	68.7	0.67	29.7	0.93

All listed samples also contained Cu metal. Its composition is given only when at least 0.1 mol.% Zn in metal could be detected

*Willemite (Zn_2SiO_4)-covered tridymite crucible

**All subsolidus experiments were premelted above solidus, so that > 50% liquid was expected to form. No remaining liquid slag was found, that means crystallization was complete. This fulfilled the main purpose of these experiments—bracketing the invariant temperatures from the below

is deduced from the steep zincite liquidus. This range is difficult to confirm due to high volatility of Zn. Solubility of ZnO in Cu-rich slag rapidly increases on addition of SiO_2, and zincite primary phase field is replaced by willemite and later tridymite. The curvature of isotherms in the tridymite and cristobalite phase fields towards higher SiO_2 in the central area of the triangle indicates strong negative interaction energy between ZnO and "$CuO_{0.5}$" in the silicate solution, opposite to what is observed in SiO_2-free solutions. This stabilization of solutions along the ZnO·$CuO_{0.5}$-SiO_2 line becomes so significant above 1600 °C that the areas of two liquids in the "$CuO_{0.5}$"-SiO_2 and ZnO-SiO_2 binaries disappear towards the 1:1 Cu:Zn ratio. This makes the present system an example of importance to study ternary systems in wide ranges of compositions, as their properties cannot be accurately

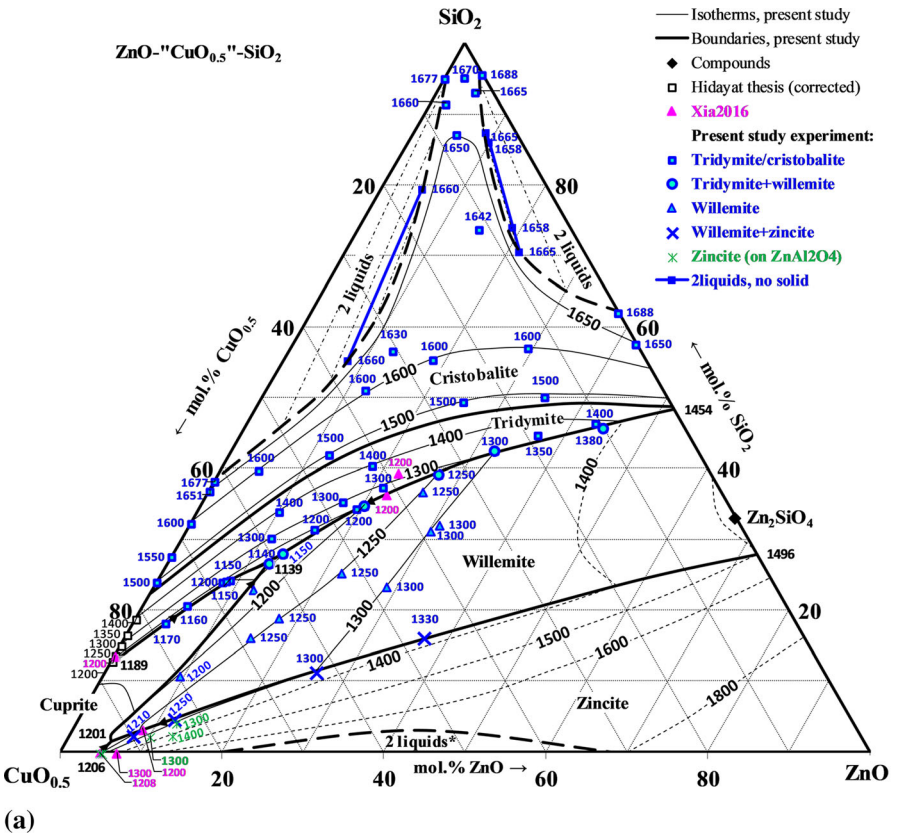

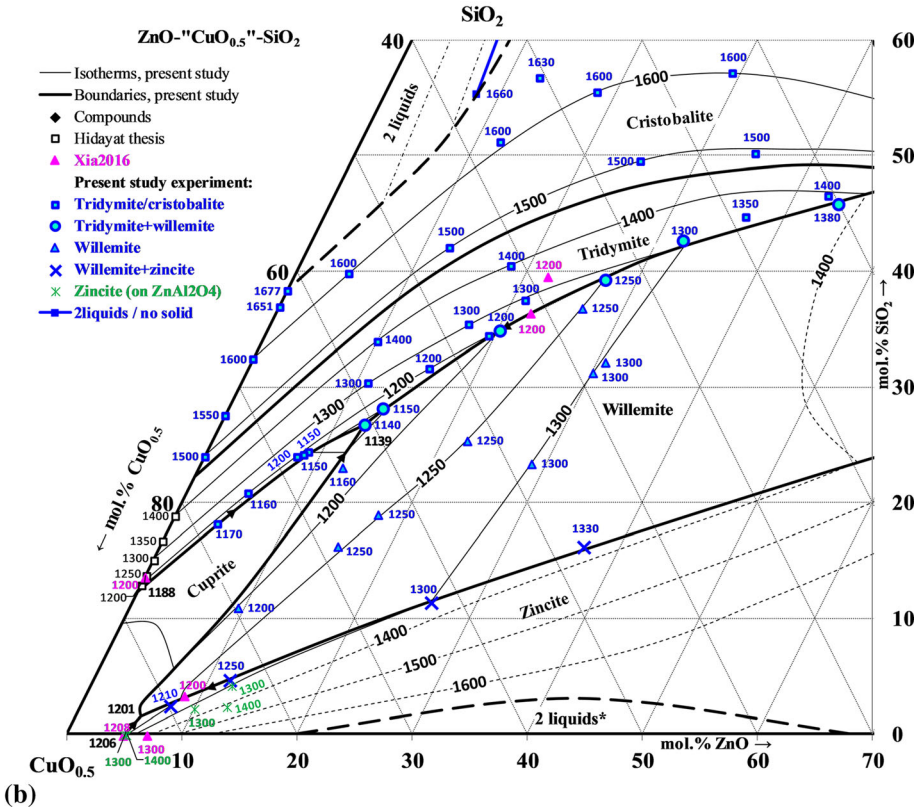

Fig. 2 Liquidus points of the ZnO-"$CuO_{0.5}$"-SiO_2 system in equilibrium with metal, compared to literature data by Xia et al.[2] and Hidayat[17]: (a) complete diagram, (b) zoomed Cu-rich area. Points on "$CuO_{0.5}$"-SiO_2 and ZnO-SiO_2 binaries have been also reported in Ref [14,16]. Isotherms and boundaries are drawn using the present experimental points (where available) or estimated with a preliminary thermodynamic model. *There is no direct experimental confirmation for two liquids existence in the ZnO-"$CuO_{0.5}$" system, it is suggested based on extrapolation of low-temperature data

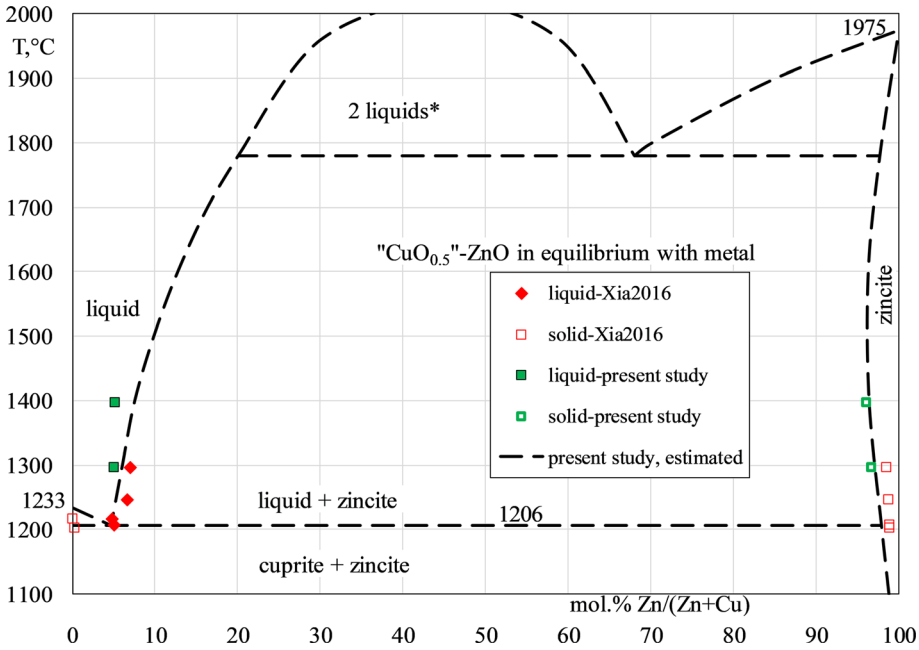

Fig. 3 Liquidus points of the ZnO-"$CuO_{0.5}$" system in equilibrium with metal, compared to literature data by Xia et al.[2] *There is no direct experimental confirmation for two liquids existence in the ZnO-"$CuO_{0.5}$" system, it is suggested based on extrapolation of low-temperature data

predicted from the limiting binaries—in this case, three systems with positive interactions combine into a ternary with negative interactions, and miscibility gaps disappear.

The combination of cristobalite and two immiscible liquids exists in many ternary systems over a range of temperatures. It is not prohibited by Gibbs rule. Unlike the binary system, a small change in temperature does not destroy such phase assemblage: a new equilibrium will be established on another tieline between two immiscible liquids, with change in proportion of two liquids and cristobalite. Examples of this phase assemblage were recently published by the authors.[14,20] There is no need to assume constant diffusion of SiO_2. Moreover, the experiments in the manuscript were indeed measured at variable distances from the substrate (30-500 micron), and no significant variation in compositions of liquids were detected.

In the $CuO_{0.5}$-SiO_2 and ZnO-SiO_2 binaries, the structures corresponding to monotectic temperatures (1677 °C and 1688 °C, respectively) are metastable and one phase is expected to disappear within much longer time (that was unpractical to use due to high failure risk of the furnace and substrate at these high temperatures). The gradients in composition of the phases were within only 0.3% ($CuO_{0.5}$-SiO_2) and 0.6% (ZnO-SiO_2). This indicates that the real monotectic temperatures are very close to the experimental temperatures (possible 5 °C uncertainty including the uncertainty of the furnace controller and thermocouple).

4 Conclusions

Phase equilibria of the ZnO-"$CuO_{0.5}$" and ZnO-"$CuO_{0.5}$"-SiO_2 systems in equilibrium with Cu-Zn metal at liquidus have been investigated at 1403-1948 K (1130-1675 °C). Tridymite, cristobalite, willemite, zincite, cuprite and two immiscible liquids fields have been identified in the wide range of compositions. The obtained results will be used for development of multicomponent thermodynamic database for copper, lead and zinc pyrometallurgy.

Acknowledgments The authors would like to thank Nyrstar (Australia), Outotec Pty Ltd (Australia), Aurubis AG (Germany), Umicore NV (Belgium), and Kazzinc Ltd, Glencore (Kazakhstan), and Australian Research Council Linkage project LP150100783 for their financial support for this research. The authors are grateful to Prof. Peter C. Hayes (UQ) for valuable comments and suggestions, to Ms. Suping Huang, Mr. Shuyi Lou, Mr. Ryan Wright for assistance with conducting experiments, and to the staff of the University of Queensland Centre for Microanalysis and Microscopy (CMM) for their support in maintenance and operation of scanning and electron microprobe facilities in the Centre.

References

1. L. Xia, Z. Liu, and P.A. Taskinen, Phase Equilibria Study of Cu–O–ZnO System in Various Oxygen Partial Pressures, *Ceram. Int.*, 2016, **42**(4), p 5418-5426

2. L. Xia, Z. Liu, P.A. Taskinen, Experimental Determination of the Liquidus Surface (1473 k) in Cu–ZnO–SiO_2–O System at Various Oxygen Partial Pressures, in *Advances in Molten Slags, Fluxes, and Salts: Proceedings of the 10th International Conference on Molten Slags, Fluxes and Salts (MOLTEN16)*, TMS (The Minerals, Metals & Materials Society, 2016), pp 971–978
3. L. Xia, Z. Liu, and P. Taskinen, Experimental Determination of the Liquid Phase Domain of the Cu–O–ZnO–SiO_2 System in Equilibrium with Air, *Can. Metall. Q.*, 2017, **56**(1), p 10-17
4. T. Hidayat, H.M. Henao, P.C. Hayes, and E. Jak, Phase Equilibria Studies of the Cu–Fe–O–Si System in Equilibrium with Air and with Metallic Copper, *Metall. Mater. Trans. B*, 2012, **43**, p 1034-1045
5. E. Jak, P.C. Hayes, and H.-G. Lee, Improved Methodologies for the Determination of High Temperature Phase Equilibria, *Korean J. Miner. Mater. Inst. (Seoul)*, 1995, **1**(1), p 1-8
6. E. Jak, Integrated Experimental and Thermodynamic Modelling Research Methodology for Metallurgical Slags with Examples in the Copper Production Field, in *9th International Conference on Molten Slags, Fluxes and Salts (MOLTEN12)*, W077 (The Chinese Society for Metals, Beijing, China, 2012).
7. C. Landolt, *Equilibrium Studies in the System Copper–Silicon–Oxygen*, Ph.D. Thesis, Pennsylvania State University, 1969
8. J. Philibert, Method for Calculating the Absorption Correction in Electron-probe Microanalysis, in *3rd International Symposium on X-ray Optics and X-ray Microanalysis* (Stanford University, 1963), pp. 379–392
9. P. Duncumb, S.J.B. Reed, *Calculation of Stopping Power and Backscatter Effects in Electron Probe Microanalysis* (1968)
10. P. Duncumb, Quantitative Electron Probe Microanalysis, in *25th Anniversary Meeting of the Electronmicroscopy and Analysis* (1971), pp. 132–137
11. M. Shevchenko and E. Jak, Experimental Liquidus Studies of the Pb–Fe–Si–O System in Equilibrium with Metallic Pb, *Metall. Mater. Trans. B*, 2018, **49**(1), p 159-180
12. M. Shevchenko and E. Jak, Experimental Phase Equilibria Studies of the PbO–SiO_2 System, *J. Am. Ceram. Soc.*, 2017, **101**(1), p 458-471
13. M. Shevchenko, J. Chen, E. Jak, Establishing Additional Correction for Quantitative EPMA Measurements in the System PbO–SiO_2, in *AMAS 2017, 14th Biennial Australian Microbeam Analysis Symposium*, 6–10 February (Brisbane, QUT, Australia, 2017), pp. 94–95
14. M. Shevchenko and E. Jak, Experimental Liquidus Studies of the Binary Pb–Cu–O and Ternary Pb–Cu–Si–O Systems in Equilibrium with Metallic Pb–Cu Alloys, *J. Phase Equilib. Diffus.*, 2019, **40**(5), p 671-685
15. M. Shevchenko and E. Jak, Experimental Liquidus Study of the Binary PbO–ZnO and Ternary PbO–ZnO–SiO_2 Systems, *Ceram. Int.*, 2019, **45**(6), p 6795-6803
16. M. Shevchenko and E. Jak, Experimental Liquidus Study of the Ternary CaO–ZnO–SiO_2 System, *Metall. Mater. Trans. B*, 2018, **50**(6), p 2780-2793
17. T. Hidayat, *Equilibria Study of Complex Silicate-Based Slag in the Copper Production*, PhD thesis, The University of Queensland, 2013
18. S. Nikolic, P.C. Hayes, and E. Jak, Experimental Techniques for Investigating Calcium Ferrite Slags at Metallic Copper Saturation and Application to the Systems "Cu_2O"–"Fe_2O_3" and "Cu_2O"–CaO at Metallic Copper Saturation, *Metall. Mater. Trans. B*, 2009, **40B**(6), p 892-899
19. M. Shevchenko and E. Jak, Experimental Liquidus Studies of the Zn–Fe–Si–O System in Air, *Int. J. Mater. Res. (IJMR)*, 2019, **110**(7), p 600-607
20. M. Shevchenko and E. Jak, Experimental Liquidus Studies of the Pb–Fe–Si–O System in Air, *J. Phase Equilib. Diffus.*, 2019, **40**(3), p 319-355